



1 Spatio-temporal patterns of the effects of precipitation variability  
2 and land use/cover changes on long-term changes in sediment yield  
3 in the Loess Plateau, China

4  
5 Guangyao Gao<sup>1,2</sup>, Bojie Fu<sup>1,2</sup>, and Murugesu Sivapalan<sup>3,4</sup>

6  
7 <sup>1</sup>State Key Laboratory of Urban and Regional Ecology, Research Center for  
8 Eco-Environmental Sciences, Chinese Academy of Sciences, Beijing 100085, China

9 <sup>2</sup>Joint Center for Global Change Studies, Beijing 100875, China

10 <sup>3</sup>Department of Geography and Geographic Information Science, University of Illinois at  
11 Urbana-Champaign, Champaign, Illinois, USA

12 <sup>4</sup>Department of Civil and Environmental Engineering, University of Illinois at  
13 Urbana-Champaign, Urbana, Illinois, USA

14  
15 *Correspondence to:* Guangyao Gao (gygao@rcees.ac.cn)

16  
17 **Abstract**

18 Within China's Loess Plateau there have been concerted revegetation efforts and  
19 engineering measures over the last 50 years aimed at reducing soil erosion and land  
20 degradation. As a result, annual streamflow, sediment yield and sediment concentration  
21 have all decreased considerably. Human induced land use/cover change (LUCC) was the  
22 dominant factor, contributing over 70% of the sediment load reduction, with reductions of  
23 annual precipitation contributing the remaining 30%. In this study, we use data on 50-year  
24 time series (1961-2011), showing decreasing trends in the annual sediment loads of fifteen



25 catchments, to generate spatio-temporal patterns in the effects of LUCC and precipitation  
26 variability on sediment yield. The space-time variability of sediment yield was expressed as  
27 a product of two factors representing: (i) effect of precipitation (spatially variable) and (ii)  
28 fraction of treated land surface area (temporally variable). Under minimal LUCC, annual  
29 sediment yield varied linearly with precipitation, with the precipitation-sediment load  
30 relationship showing coherent spatial patterns amongst the catchments. On the other hand,  
31 the effect of LUCC is expressed in terms of a sediment coefficient, i.e., ratio of annual  
32 sediment yield to annual precipitation, which is equivalent to the slope of the sediment  
33 yield-precipitation relationship. Sediment coefficients showed a steady decrease over the  
34 study period, following a linear decreasing function of the fraction of treated land surface  
35 area. In this way, the study has brought out the separate roles of precipitation variability  
36 and LUCC in controlling spatio-temporal patterns of sediment yield at catchment scale.

37

38 **Keywords:** Loess Plateau, sediment yield, land use/land cover change, climate change,  
39 precipitation variability

40

## 41 **1 Introduction**

42 Streamflow and sediment transport are important controls on biogeochemical processes  
43 that govern ecosystem health in river basins (Syvitski, 2003). Changes in soil erosion on  
44 landscapes and the resulting changes in sediment transport rates in rivers have great  
45 environmental and societal consequences, particularly since they can be brought about by  
46 climatic changes and human induced land use/cover changes (LUCC) (Syvitski, 2003;



47 Beechie et al., 2010). Understanding the dominant mechanisms behind such changes at  
48 different time and space scales is crucial to the development of strategies for sustainable  
49 land and water management in river basins (Wang et al., 2016).

50 In recent decades, streamflows and sediment yields in large rivers throughout the world  
51 have undergone substantial changes (Milly et al., 2005; Nilsson et al., 2005; Milliman et al.,  
52 2008; Cohen et al., 2014). Notable decreases in sediment yields have been observed in  
53 approximately 50% of the world's rivers (Walling and Fang, 2003; Syvitski et al., 2005).

54 Many studies have investigated the dynamics of streamflows and sediment yields at  
55 different spatial and temporal scales (Mutema et al., 2015; Song et al., 2016; Gao et al.,  
56 2016; Tian et al., 2016). In addition to climate variability, LUCC, soil and water

57 conservation measures (SWCM) and construction of reservoirs and dams have substantially  
58 contributed to the sediment load reductions (Walling, 2006; Milliman et al., 2008; Wang et  
59 al., 2011). While previous studies have certainly provided valuable insights into the

60 streamflow and sediment load changes, the distinctive roles of LUCC and precipitation  
61 variability in changing sediment loads still need further investigation in large domains and  
62 across gradients of climate and land surface conditions (Walling, 2006; Mutema et al.,

63 2015). A particularly useful approach to the development of generalizable understanding of  
64 the effects of precipitation variability and LUCC is a comparative analysis approach

65 focused on extracting spatio-temporal patterns of sediment yields based on observations in  
66 multiple locations within the same region, or even across different regions. This is

67 especially valuable and crucial in areas with severe soil erosion and fragile ecosystems, e.g.,  
68 the Loess Plateau (LP) in China. This is the motivation for the work presented in this paper.



69 The LP lies in the middle reaches of the Yellow River (YR) Basin, and contributes  
70 nearly 90% of the YR sediment (Wang et al., 2016). The historically severe soil erosion in  
71 the LP is due to sparse vegetation, intensive rainstorms, erodible loessial soil, steep  
72 topography and a long agricultural history (Rustomji et al., 2008). To control such severe  
73 soil erosion, several SWCM including terrace and check-dam construction, afforestation  
74 and pasture reestablishment have been implemented since the 1950s (Yao et al., 2011; Zhao  
75 et al., 2016). A large ecological restoration campaign, the Grain-for-Green (GFG) project  
76 by converting farmland on slopes exceed 15° to forest and pasture lands, was implemented  
77 in 1999 (Chen et al., 2015). Furthermore, the climate in the LP region has been showing  
78 both warming and drying trends (i.e., increased potential evapotranspiration and reduced  
79 precipitation) since the 1950s (Zhang et al., 2016).

80 These substantial LUCC have notably altered the hydrological regimes in the LP  
81 combined with the climate change. Consequently, the sediment yields within the LP have  
82 showed a predictable decline trend over the past 60 years (Zhao et al., 2016), resulting in  
83 approximately a 90% decrease of sediment yield in the YR (Miao et al., 2010, 2011; Wang  
84 et al., 2016). Many other studies have detected the influences of LUCC and precipitation  
85 variability on sediment load changes within the LP. Rustomji et al. (2008) estimated that  
86 the contributions of catchment management practices to the decrease of annual sediment  
87 yield ranged between 64% and 89% for eleven catchments in the LP during 1950s-2000.  
88 Zhao et al. (2016) examined the spatio-temporal variation of sediment yield from 1957 to  
89 2012 across the LP. Zhang et al. (2016) pointed out that the combined effects of climate  
90 aridity, engineering projects and vegetation cover change have induced significant



91 reductions of sediment yield between 1950 and 2008. Wang et al. (2016) found that  
92 engineering measures for soil and water conservation were the main factors for the  
93 sediment load decrease between 1970s-1990s, but large-scale vegetation restoration  
94 campaigns also played important role in reducing soil erosion since the 1990s.

95 In terms of the results of these previous studies, it is now generally accepted that the  
96 largest reductions of sediment yield within the LP were resulted from LUCC. However, this  
97 is general knowledge covering the whole region, and given the significant variability of  
98 climate and catchment characteristics across the LP (Sun Q et al., 2015; Sun W et al., 2015),  
99 it is important to go further and explore how these might affect spatio-temporal patterns of  
100 sediment yield. Exploration of these patterns is important for sustainable ecosystem  
101 restoration and water resources planning and management within the LP. They also will  
102 serve as the basis for future research aimed at the development of more generalizable  
103 understanding of landscape and climate controls on sediment yields at the catchment scale.

104 The specific objectives of this study therefore are to: (1) attribute the temporal changes  
105 in sediment yield to changes in both precipitation variability and LUCC over the entire  
106 study period (1961-2011) within the middle part of the LP, (2) extract spatio-temporal  
107 trends in sediment yields on the basis of annual sediment yield data from 15 catchments  
108 within the region, (3) separate the contributions of precipitation variability and fractional  
109 area of LUCC to the observed spatio-temporal patterns of sediment yields, and pave the  
110 way for more detailed process-based studies in the future.

## 111 **2 Materials and methods**

### 112 **2.1 Study area**



113 This study is conducted in the central region of the LP, from the Toudaoguai to Longmen  
114 hydrological stations in the mainstream of the YR (Fig. 1). This area is usually referred to  
115 as the Coarse Sandy Hilly Catchments (CSHC) region. The main stream that flows through  
116 the CSHC region is 733 km long and covers an area of  $12.97 \times 10^4$  km<sup>2</sup>. The CSHC region  
117 accounts for 14.8% of the entire YR Basin, but supplies over 70% of total sediment load in  
118 the YR, especially coarse sand (Rustomji et al., 2008). The CSHC region is characterized  
119 by arid to semi-arid climate conditions. The annual precipitation in the CSHC region during  
120 1961-2011 is 437 mm on average, and varied from 580 mm in the southeast to lower than  
121 300 mm in the northwest (McVicar et al., 2007). The precipitation that occurs during the  
122 flood season (June-September) is usually in the form of rainstorms with high intensity and  
123 accounts for 72% of the annual rainfall total. Correspondingly, about 45% of the annual  
124 runoff and 88% of the annual sediment yield within the CSHC region are produced during  
125 the flood season. The northwestern part of the CSHC is relatively flat while the  
126 southeastern part is more finely dissected (Rustomji et al., 2008).

127 Fourteen main catchments along the north-south transect within the CSHC study area  
128 were chosen for study (Fig. 1). These catchments account for 57.4% of the CSHC area, and  
129 contribute about 70% and 72% of streamflow and sediment load of the overall CSHC,  
130 respectively. Characteristics of these catchments are shown in Table 1. It can be seen that  
131 the catchments present strong climate and land surface gradients. The catchments in the  
132 northwestern part (#1-6) have relatively lower mean annual precipitation ( $380 \text{ mm} < \bar{P} < 445$   
133 mm, where  $\bar{P}$  is mean annual precipitation over 1961-2011) and low vegetation cover  
134 ( $0.32 < \text{LAI} < 0.37$ , where LAI is the leaf area index), while the corresponding values for



135 catchments in the southeastern part (#7-14) are 470-570 mm and  $0.63 < LAI < 2.16$ ,  
136 respectively. The entire CSHC region is considered as an additional “catchment” and it is  
137 also examined. The streamflow and sediment load for the whole CSHC region was equal to  
138 the differences of value between the Toudaoguai and Longmen gauging station. Fig. 2  
139 shows the changes of annual precipitation, streamflow and sediment load for the whole  
140 CSHC region during 1961-2011.

## 141 2.2 Data

142 Monthly streamflow and sediment load data during 1961-2011 were provided by the  
143 Yellow River Conservancy Commission of China. Daily rainfall data from 1961 to 2011 at  
144 66 meteorological stations in and around the CSHC region were obtained from the National  
145 Meteorological Information Center of China. The spatially average of rainfall data were  
146 determined by the co-kriging interpolation algorithm with input of the DEM. With the  
147 hydro-meteorological data, annual precipitation,  $P$  [mm], streamflow,  $Q$  [mm], specific  
148 sediment yield defined as  $SSY = S/A$  [ $t\ km^{-2}$ ], where  $S$  is sediment load,  $t$ ,  $A$  is the drainage  
149 area of the hydrological station,  $km^2$ , sediment concentration defined as  $SC = S/(Q \cdot A)$  [ $kg$   
150  $m^{-3}$ ] and the sediment coefficient defined as  $C_s = SSY/P$  [ $t\ km^{-2}\ mm^{-1}$ ] for each catchment  
151 were estimated.

152 The land use information as at 1986, 1997 and 2010 was determined with Landsat TM  
153 remote sensing images at a spatial resolution of 30 m. Six land use types were classified,  
154 i.e., forestland, cropland, grassland, construction land, water body, and wasteland. The  
155 annual LAI data during 1982-2011 were obtained from the Global Inventory Modelling and  
156 Mapping Studies-Advanced Very High Resolution Radiometer (GIMMS AVHRR) data set



157 (<http://www.glc.f.umd.edu/data/lai/>) which has a spatial resolution of 8 km (resampled to 1  
158 km) and temporal frequencies of 15 day. Vegetation cover in the summer or autumn of  
159 1978, 1998 and 2010 was determined with Landsat MSS, Landsat TM and HJ CCD which  
160 has a spatial resolution of 56 m, 30 m and 30 m, respectively. The total areas impacted by  
161 the various SWCM (i.e., afforestation, grass plantation, terraces and check-dams)  
162 during 1960s-2000s were obtained from Yao et al. (2011).

### 163 **2.3 Methods**

#### 164 **2.3.1 Trend test**

165 The non-parametric Mann-Kendall (M-K) test method proposed by Mann (1945) and  
166 Kendall (1975) was used to determine the significance of the trends in annual  
167 meteorological and hydrological time series. A precondition for using the MK test is to  
168 remove the serial correlation of climatic and hydrological series. In this study, the  
169 trend-free pre-whitening (TFPW) method of Yue and Wang (2002) was used to remove the  
170 auto-correlations before the trend test. A  $Z$  statistic was obtained from the M-K test on the  
171 whitened series. A negative value of  $Z$  indicates a decrease trend, and vice versa. The  
172 magnitude slope of the trend ( $\beta$ ) was estimated by (Sen, 1968; Hirsch et al., 1982):

$$173 \quad \beta = \text{Median} \left[ \frac{x_j - x_i}{j - i} \right] \quad \text{for all } i < j \quad (1)$$

174 where  $x_i$  and  $x_j$  are the sequential data values in periods  $i$  and  $j$ , respectively.

#### 175 **2.3.2 Attribution analysis of changes in sediment load**

176 The time-trend analysis method was used to determine the quantitative contributions of  
177 LUCC and precipitation variability to sediment load changes. This method is primarily  
178 designed to determine the differences in hydrological time series between different periods





179 (reference and validation periods) with different LUCC conditions (Zhang et al., 2011). In  
 180 this method, the regression equation between precipitation and sediment load is developed  
 181 and evaluated during the reference period, and the established equation is then used to  
 182 estimate sediment load during the validation period. The difference between measured and  
 183 predicted sediment loads during the validation period represents the effects of LUCC, and  
 184 the residual changes are caused by precipitation variability. The governing equations of the  
 185 time-trend analysis method can be expressed as:

$$186 \quad S_1 = f(P_1) \quad (2)$$

$$187 \quad S_2' = f(P_2) \quad (3)$$

$$188 \quad \Delta S^{\text{LUCC}} = \overline{S_2} - \overline{S_2'} \quad (4)$$

$$189 \quad \Delta S^{\text{Pre}} = (\overline{S_2} - \overline{S_1}) - \Delta S^{\text{LUCC}} \quad (5)$$

190 where  $S'$  is the predicted sediment load, subscripts 1 and 2 indicate the reference and  
 191 validation periods, respectively.  $\overline{S_1}$  and  $\overline{S_2}$  represent mean measured sediment load during  
 192 the reference and validation periods, respectively, and  $\overline{S_2'}$  represents mean predicted  
 193 sediment load during the validation period.  $\Delta S^{\text{LUCC}}$  and  $\Delta S^{\text{Pre}}$  are sediment load changes  
 194 during the validation period associated with LUCC and precipitation variability,  
 195 respectively.

196 In this study, the full data period of 1961-2011 was divided into three phases  
 197 (1961-1969, 1970-1999 and 2000-2011). The first period was considered the reference  
 198 period as the effects of human activities were slight and could be mostly ignored (Wang et  
 199 al., 2016). A linear function was used to develop precipitation-sediment load relationship  
 200 during the reference period. During the second stage, numerous SWCM were implemented.



201 For the third stage, a large ecological restoration campaign (GFG project) was launched in  
202 1999.

### 203 **3 Results and discussion**

#### 204 **3.1 Changes of land use/cover**

205 The CSHC region has undergone extensive LUCC caused by the implementation of  
206 SWCM and vegetation restoration projects (e.g., the GFG project). Fig. 3a shows the  
207 distribution of land use types of the CSHC region in 1986, 1997 and 2010. More than 90%  
208 of the whole area is occupied by the cropland, forestland and grassland. The area of  
209 cropland decreased by 19.47% and forestland increased by 59.65%, and there was no  
210 obvious change for the area of grassland from 1986-2010. The majority of changes  
211 occurred during 1997-2010 due to the GFG (reforestation) project (18.58% decrease and  
212 40.71% increase for cropland and forestland, respectively). From 1986 to 2010, the water  
213 body area increased by 88.05% due to construction of reservoirs, and construction land  
214 increased by about twenty times because of the urbanization and extensive infrastructure  
215 construction.

216 The SWCM implemented in the LP included both biotic treatment (e.g., afforestation  
217 and grass-planting) and engineering measures (e.g., construction of terrace and check-dam  
218 and gully control projects). Afforestation, grass-planting and construction of terrace are the  
219 slope measures, while building of check-dams and gully control projects are the measures  
220 on the channel. Although the utilized area of engineering measures was much smaller than  
221 the biotic treatments, they can immediately and substantially trap streamflow and sediment  
222 load. The fraction of the treated area (area treated by erosion control measures relative to



223 total catchment area) within the CSHC increased from 3.95% in the 1960s to 28.61% in the  
224 2000s (Fig. 3b). The increase of the treated area was greatest during the 1980s as a result of  
225 comprehensive management of small watersheds and during the 2000s due to the GFG  
226 project since 1999. Some decreases in these areas occurred during the 1990s as some of the  
227 erosion control measures undertaken were then subsequently destroyed.

228 For the fourteen sub-catchments, vegetation cover increased from  $29.19 \pm 21.09\%$  in  
229 1978 to  $31.69 \pm 17.18\%$  in 1998, and then increased sharply to  $44.10 \pm 14.62\%$  in 2010. In  
230 the whole CSHC region, the amounts of vegetation cover in 1978, 1998 and 2010 were  
231 23.61%, 25.68% and 38.71%, respectively. The increase of vegetation cover for the  
232 catchments in the northwestern part (48.95% from 1978 to 1998 and 65.98% from 1998 to  
233 2010) was greater than that in the southeastern part (-1.48% from 1978 to 1998 and 28.72%  
234 from 1998 to 2010). The annual LAI of the fourteen sub-catchments increased by 15.50%  
235 from 1982-1999 to 2000-2011, and the relative change in the catchments of northwestern  
236 part is 27.08%, which is greater than that in the southeastern part (6.82%). For the whole  
237 CSHC region, the annual LAI changed from 0.51 during 1982-1999 to 0.55 during  
238 2000-2011, an increase of 7.31%.

### 239 3.2 Trends of hydro-meteorological and sediment yield variables

240 Table 2 shows the trends in annual  $P$ ,  $Q$ ,  $SSY$ ,  $SC$  and  $C_s$  of the fifteen catchments during  
241 1961-2011. The annual  $P$  showed a decline trend in all catchments but only significant in the  
242 Xinshui and Zhouchuan catchments ( $p < 0.05$ ). The annual  $Q$ ,  $SSY$ ,  $SC$  and  $C_s$  showed  
243 significant decreasing trends in all the catchments, and most of the decreases were at the  
244 0.001 significance level. For the fourteen sub-catchments, the average decrease rates of



245 annual values of  $Q$ ,  $SSY$ ,  $SC$  and  $C_s$  were  $0.86 \text{ mm yr}^{-1}$  ( $0.24\text{-}1.66 \text{ mm yr}^{-1}$ ),  $190.06 \text{ t km}^{-2}$   
 246  $\text{yr}^{-1}$  ( $26.47\text{-}398.82 \text{ t km}^{-2} \text{ yr}^{-1}$ ),  $2.73 \text{ kg m}^{-3} \text{ yr}^{-1}$  ( $0.69\text{-}4.70 \text{ kg m}^{-3} \text{ yr}^{-1}$ ) and  $0.38 \text{ t km}^{-2} \text{ mm}^{-1}$   
 247  $\text{yr}^{-1}$  ( $0.04\text{-}0.87 \text{ t km}^{-2} \text{ mm}^{-1} \text{ yr}^{-1}$ ), respectively. For the whole CSHC region, the  
 248 corresponding change rates of  $Q$ ,  $SSY$ ,  $SC$  and  $C_s$  were  $-0.85 \text{ mm yr}^{-1}$ ,  $-131.52 \text{ t km}^{-2} \text{ yr}^{-1}$ ,  
 249  $-2.06 \text{ kg m}^{-3} \text{ yr}^{-1}$  and  $-0.27 \text{ t km}^{-2} \text{ mm}^{-1} \text{ yr}^{-1}$ , respectively. The annual average reductions in  
 250 the whole CSHC region are equivalent to 2.56%, 3.30%, 2.01% and 3.07% of the mean  
 251 annual values of  $Q$ ,  $SSY$ ,  $SC$  and  $C_s$ , respectively.

252 The mean and the coefficient of variation,  $C_v$ , representing inter-annual variability of  
 253 annual values of  $P$ ,  $Q$ ,  $SSY$ ,  $SC$  and  $C_s$  of the fifteen catchments during the three phases  
 254 (reference period-1, period-2 and period-3) are shown in Fig. 4. Compared to the reference  
 255 period, the mean annual precipitation decreased by 11.73% (6.36-15.69%) and 10.64%  
 256 (5.88-16.7%) on average in period-2 and period-3, respectively. From period-2 to period-3,  
 257 the change of mean annual precipitation was slight (increased by 1.32% on average) with  
 258 decrease of 2.45%-5.87% in four catchments and increase in remaining catchments  
 259 (0.35%-8.29%). The variability of annual  $P$  also decreased as indicated by the reductions of  
 260  $C_v$  values during period-2 and period-3 (Fig. 4a). In contrast to annual  $P$ , the reductions of  
 261 mean annual  $Q$ ,  $SSY$ ,  $SC$  and  $C_s$  were clearly more evident. With respect to the reference  
 262 period, the reduction was 34.41% (9.45%-54.72%), 48.02% (17.98%-67.61%), 24.20%  
 263 (-9.93%-47.77%) and 39.31% (4.64%-63.5%) for  $Q$ ,  $SSY$ ,  $SC$  and  $C_s$  during period-2, and the  
 264 decreasing rate was even more in period-3 with values of 64.82% (36.72%-84.19%), 88.23%  
 265 (64.94% -97.64%), 67.81% (17.28%-91.12%) and 85.85% (63.51%-96.97%), respectively.  $C_v$   
 266 of annual  $Q$  increased in eight catchments, with the remaining ones showing decreasing



267 trends (Fig. 4b),  $C_v$  values for  $SSY$ ,  $SC$  and  $C_s$  increased in all catchments (Figs 4c-4e).

### 268 **3.3 Quantitative attribution of sediment load decline**

269 The effects of precipitation change and LUCC on sediment yield reductions in period-2 and

270 period-3 were quantified using Eqs. (2-5) and the results are shown in Fig. 5. The analysis

271 showed that both decreased precipitation and increased area treated with erosion control

272 measures contributed to the observed sediment load reduction, and that LUCC played the

273 major role. On average, the LUCC and precipitation change contributed 71.01% and

274 28.99%, respectively, to sediment load reduction from the reference period to period-2, and

275 their contributions were, respectively, 84.77% and 15.23% to sediment load reduction from

276 the reference period to period-3, respectively. The effect of LUCC in period-3 was greater

277 than that in period-2 as the land use and vegetation coverage had undergone substantial

278 changes due to the ecological restoration campaigns launched during period-3 (see Fig. 3).

279 From period-2 to period-3, the contribution of precipitation was negative for sediment yield

280 reduction in eleven catchments where the annual precipitation slightly increased during

281 these two periods, and thus the contribution of LUCC was larger than 100% (Fig. 5c). In

282 the remaining four catchments, the average contribution of LUCC increased to 86.15%.

283 In broad terms there are two factors that govern annual sediment yield of a catchment:

284 precipitation and landscape properties (soil, topography and vegetation). Higher

285 precipitation means higher streamflow, which is the immediate driver of erosion and

286 sediment transport. Landscape properties not only have an impact on the volume or

287 intensity of streamflow, but also determine the erodibility of the soil. On the basis of the

288 field evidence, we can hypothesize that the annual sediment yield  $SSY$  can be expressed as



289 a product of a spatially variable component, which is only a function of a spatially variable  
290 annual precipitation,  $P$ , and a temporally variable component, which is only a function of a  
291 temporally variable fraction of area treated with erosion control measures,  $A_c$ .

$$292 \quad \quad \quad SSY(\mathbf{x}, t) = SSY_0 \cdot f_1[P(\mathbf{x})] \cdot f_2[A_c(t)] \quad (6)$$

293 where  $SSY_0$  is the sediment yield in the reference period,  $t$  represents time and  $\mathbf{x}$  is a vector  
294 that represents spatial location of the catchments, and  $f_1$  and  $f_2$  are appropriate (yet to be  
295 determined) functional forms that reflect the net effects of sub-catchment scale and  
296 sub-annual runoff on sediment generation processes. In this framework, the variation of  
297  $SSY$  during the reference period mainly depends on precipitation, and any spatial patterns  
298 of  $SSY$  among catchments may be controlled by differences in annual precipitation and land  
299 surface conditions before LUCC took effect. As LUCC increased and took effect, the  
300 temporal changes of  $SSY$  may depend more on the fraction of treated surface area and  
301 precipitation possibly might play a secondary role. Guided by this hypothesis, we next  
302 organize the data analysis to generate separate spatial and temporal patterns that constitute  
303 the respective components of the spatio-temporal patterns.

#### 304 **3.4 Spatial pattern of the impacts of precipitation on sediment yield during Period 1**

305 The regression relationships between annual precipitation and sediment yield during the  
306 reference period are shown in Fig. 6. Most of the catchments showed strong linear  
307 correlation between precipitation and sediment yield. The coefficient of determination ( $R^2$ )  
308 ranged from 0.24 to 0.85, and the correlation was significant in eight catchments ( $p < 0.05$ )  
309 (Table 3). Furthermore, the precipitation-sediment load relationship varied from catchment  
310 to catchment and showed a spatial pattern. The correlation coefficient between precipitation



311 and sediment yield was greater for catchments in the northwestern part with average  $R^2$   
312 value of 0.69 and  $p$  value of 0.017 compared to those in the southeastern part where the  
313 average  $R^2$  and  $p$  values were 0.36 and 0.118, respectively (Table 3). Based on the slopes of  
314 the regression equations between annual precipitation and sediment yield, the fifteen  
315 catchments were classified into four groups, which indicate that the sediment production  
316 capability of annual precipitation is different among the catchments (Fig. 6). The three  
317 catchments of the first group in Fig. 6a had the greatest slopes (85-95) and the Shiwang  
318 catchment in Fig. 6d had the lowest slope of 7.26. The average slope of the five catchments  
319 in Group-2 was 57.57 (50-70), and the slope value of the six catchments in Group-3 was  
320 30.88 (20-40). Overall, the regressed linear equations were significant for most of the  
321 catchments, and were suitable for estimating the relative contributions of LUCC and  
322 precipitation variability to sediment load changes.

323 Differences in catchment characteristics, including land use/cover, soil properties and  
324 topography, as well as precipitation characteristics, are clearly the reason for the spatial  
325 patterns in the precipitation-sediment yield relationship (Morera et al., 2013; Mutema et al.,  
326 2015). To fully explore this, the mapping of information of catchment characteristics into  
327 sediment yield models and simulating under climate scenarios is needed (Ma et al., 2014;  
328 Achete et al., 2015). In this context, the inter-annual and intra-annual patterns of variability  
329 of precipitation, including the distribution of storm events, may also contribute to the  
330 observed spatial patterns of precipitation-sediment yield relationship.

### 331 **3.5 Spatial pattern of precipitation impacts on sediment yield during Periods 2 and 3**

332 Precipitation is the primary driver of runoff and, therefore, directly influences the sediment



333 transport capacity of streamflow and sediment yield at the catchment scale. Compared to  
334 the reference period, the correlation between precipitation and sediment yield during the  
335 period-2 decreased in the catchments, as indicated by the reductions of  $R^2$  value in Table 3  
336 and the increased scatter of the linear relationship in Fig. 7. The slope of the regression line  
337 in the period-2 decreased in most of the catchments with respect to the reference period,  
338 but in some catchments (e.g., Huangfu, Gushan and Kuye) the reduction in the slope was  
339 slight. Furthermore, the precipitation-sediment yield relationship during these two periods  
340 showed a similar spatial pattern. In period-2, the fifteen studied catchments could also be  
341 classified into four groups using the decrease of slope of the regression line from Group-1  
342 to Group-4 (Fig. 7). From the reference period to period-2, only Jialu catchment moved  
343 from Group-1 to Group-2 and Yanhe catchment moved from Group-2 to Group-3 (Figs. 6  
344 and 7).

345 In period-3, the correlation between precipitation and sediment yield was much weaker  
346 compared to that during the reference period and period-2 (Table 3 and Fig. 8). The  
347 relationship between precipitation and sediment yield was non-significant in all the  
348 catchments (Table 3), and the scatter of the data points in Fig. 8 was notable. The slope of  
349 the regression line during period-3 decreased sharply (Table 3), and for some catchments  
350 the slope was even negative (Fig. 8d). This result indicates that the sediment production  
351 capability of annual precipitation reduced greatly during period-3, and the increase of  
352 precipitation amount in some catchments did not lead to an increase of sediment yield.  
353 Furthermore, the spatial pattern of precipitation-sediment relationship during period-3 was  
354 much different from that during the reference period and during period-2 through





355 comparisons of Fig. 8 with Figs. 6-7. As shown in Fig. 8, most of the catchments were  
356 distributed in Group-1 and Group-4, which displayed considerable variability in the  
357 precipitation-sediment relationship among the catchments.

358 The aforementioned analysis of precipitation-sediment yield relationship in different  
359 periods clearly indicates that the impacts of precipitation on sediment load declined with  
360 time, and the impacts were different among catchments, with a clear spatial pattern. The  
361 decreased effects of precipitation on sediment load were consistent with the significant  
362 reductions of sediment coefficient (Table 2) and the decreased contribution of precipitation  
363 to sediment load reduction (28.99% and 15.23% in period-2 and period-3, respectively).  
364 During period-2, the LUCC were mainly induced by SWCM, especially engineering  
365 measures. During period-3, the combined effects of substantial vegetation cover and  
366 conservation measures undoubtedly further weakened the effects of precipitation on  
367 sediment load reduction.

368 As LUCC took effect during period-2 and period-3, and despite the much reduced role  
369 of precipitation in driving changes in sediment yield, within-year temporal rainfall patterns  
370 did play an important role in the observed changes of sediment yield, given that most of the  
371 sediment yield was produced during a few key storm events. Taking the Yanhe catchment  
372 as an example, the precipitation amount during the rainy season (May-October when  
373 sediment load was measured) in 2003 and 2004 was 514.31 mm and 389.05 mm,  
374 respectively, whereas the sediment load in 2004 ( $2427.37 \times 10^4$  t) was about over four times  
375 of that in 2003 ( $590.04 \times 10^4$  t). As shown in Fig. 9, there were six days with precipitation  
376 amount over 20 mm and the maximum daily precipitation amount on 25th Aug was 27.85



377 mm in 2003, and the values in 2004 were five days and 46.34 mm on 10th Aug.  
378 Furthermore, heavy rainfall events were distributed in every month in 2003, whereas they  
379 were concentrated in July and August in 2004. There were five evident peaks of sediment  
380 load with the sum of  $1646.24 \times 10^4$  t (67.82% of annual total) in 2004, especially the one on  
381 10th Aug produced  $784.53 \times 10^4$  t sediment load (32.32% of annual total) (Fig. 9b). In  
382 contrast, there were three peaks of sediment load in 2003, and the maximum value was  
383 only  $139.97 \times 10^4$  t (Fig. 9a). Therefore, apart from annual precipitation amounts,  
384 within-year rainfall patterns should also be considered to investigate the effects of  
385 precipitation on temporal-spatial changes of streamflow and sediment load.

### 386 **3.6 Spatial pattern of the impacts of land use/cover on sediment load change**

387 The sediment load reductions in the LP were primarily caused by the LUCC and the  
388 implementation of SWCM. The cropland area decreased  $6233.13 \text{ km}^2$  (5.54% of region area)  
389 and the forestland area increased  $7246.45 \text{ km}^2$  (6.44% of region area) from 1986 to 2010.  
390 Most of the increase in forestland area was converted from cropland area induced by the GFG  
391 or reforestation project. As a result of the land use change, vegetation cover increased greatly  
392 and it substantially contributed to the decreases of runoff and sediment production. The  
393 SWCM, such as afforestation and engineering measures were the major interventions in the  
394 study area to retain precipitation and consequently reduce streamflow and sediment load.  
395 Establishing perennial vegetation cover was considered as one of the most effective measures  
396 to stabilize soils and minimize erosion (Farley et al., 2005; Liu et al., 2014). It was reported  
397 that both runoff coefficient and sediment concentration of catchments in the LP decreased  
398 significantly and linearly with the vegetation cover (Wang et al., 2016). The engineering



399 structures mainly included creation of terrace and building of check-dams and reservoirs,  
400 which reduced flood peaks and stored water and sediment within the catchment. There were  
401 about 110, 000 check-dams in the LP which trapped about 21 billion m<sup>3</sup> of sediment during  
402 the past six decades (Zhao et al., 2016). Over time, the effectiveness of engineering measures  
403 decreased as they progressively fill with sediments, and vegetation restoration must in future  
404 play a greater role in control of soil erosion for the LP.

405 To quantify the effects of SWCM on sediment load reduction, the relationship between  
406 the sediment coefficient and the fraction of area treated with erosion control measures in the  
407 15 catchments was analysed and the results are presented in Fig. 10. The sediment coefficient  
408 decreased linearly with the fraction of treated land surface area in all catchments. The  
409 correlation was significant in eleven catchments ( $p < 0.05$ ) with  $R^2$  ranging from 0.78 to 0.99  
410 (Table 4). Note that the temporal variations presented in Figure 10 are not based on annual  
411 data (such data does not exist), but longer-term (decadal) averages.

412 The effects of SWCM on sediment load change show a spatial pattern. The correlation  
413 between sediment coefficient and conservation measures was stronger in catchments located  
414 in the north-western part compared to that in the south-eastern part (Table 4). Based on the  
415 slope of the regression equation between the sediment coefficient and fraction of the treated  
416 area, the 15 catchments were classified into three groups (Fig. 10), which indicated that the  
417 degree of sediment load impacted by conservation measures was different among the  
418 catchments. The four catchments of the first group in Fig. 10a had the greatest slopes over  
419 0.85, followed by the four catchments in Group-2 (0.50–0.65) and seven catchments in  
420 Group-3 (less than 0.30). Finally, inspired by the hypothesis presented in Eq. 6 and on the



421 basis of the observed linear relationships, it is now plausible to construct an empirical  
422 relationship between a decadal average of sediment yield and the combination of decadal  
423 average precipitation,  $\bar{P}$ , and the area under land use/cover change,  $A_c$ , of the following  
424 form:

$$425 \quad SSY = k_0 \bar{P} (1 - k_1 A_c) \quad (7)$$

#### 426 **4 Conclusions**

427 The LP has undergone major changes in land use/land cover over the last 50 years as part  
428 of a concerted effort to cut back on soil erosion and land degradation and sediment yield of  
429 rivers. These included terrace and check-dam construction, afforestation, and pasture  
430 reestablishment. Over the same period the region has also experienced some reduction in  
431 rainfall, although this is relatively insignificant. Through analyses of hydrological and  
432 sediment transport data, this study has brought out the long-term decreasing trends in  
433 sediment loads across fifteen large sub-catchments located in the region. The study was  
434 particularly aimed at extracting spatio-temporal patterns of sediment yield and attributing  
435 these patterns to the broad hydro-climatic and landscape controls.

436 Over the study period (1961-2011), the total area undergoing erosion control treatment  
437 went up from only 4% to over 30%. This included to decrease of cropland by 20%, increase  
438 of forestland of 60% over the 40 years (grasslands remained unchanged), and an increase in  
439 water body area by 90% (through the building of reservoirs). Over the same period annual  
440 precipitation decreased by not more than 10%. As a result of the erosion control measures,  
441 over the entire 50-year period, there have been major reductions in streamflow (65%),  
442 sediment yield (88%), sediment concentration (68%) and sediment efficiency, i.e., annual



443 sediment yield/annual precipitation (86%).

444 The observed data in the 15 study catchments also exhibits interesting spatio-temporal  
445 patterns in sediment yield. The study attempted to separate the relative contributions of  
446 annual precipitation and LUCC to these spatio-temporal patterns. Before LUCC took effect  
447 the data indicates a linear relationship between annual sediment yield and annual  
448 precipitation in all 15 catchments, with highly variable slopes of the relationship between  
449 the catchments, which exhibited systematic spatial patterns, in spite of considerable scatter.  
450 As LUCC increased and took effect, the scatter increased and the slopes of the sediment  
451 yield vs precipitation relationship became highly variable and lost any predictive power.  
452 The study then looked at the controls on sediment coefficient instead of sediment yield  
453 (thus eliminating the effect of precipitation and enabling a direct focus on landscape  
454 controls). The results of this analysis found that sediment coefficient was heavily  
455 dependent on the area under land use/cover treatment, exhibiting a linear (decreasing)  
456 relationship. Even here, there was a considerable variation in the slope of the relationship  
457 between the 15 catchments, which exhibited a systematic spatial pattern.

458 Preliminary analyses presented in this study suggests that much of the sediment yield in  
459 the LP may be caused during only a few major storms. Therefore, the seasonality and  
460 intra-annual variability of precipitation may play important roles in annual sediment yield,  
461 which may also explain the spatial patterns of sediment yield and the effects of the various  
462 LUCC. Also, the precipitation threshold for producing sediment yield would have increased  
463 greatly as a result of SWCM and vegetation restoration in the LP. Exploration of these  
464 questions in detail will require a more physically based model that can account for fine



465 scale rainfall variability. This is the next immediate step in our investigations, and will be  
466 reported on in the near future.

467

#### 468 **Acknowledgements**

469 This research was funded by the National Natural Science Foundation of China (41390464  
470 and 41471094), the Chinese Academy of Sciences (GJHZ 1502) and the Youth Innovation  
471 Promotion Association CAS (2016040). We thank the Ecological Environment Database of  
472 Loess Plateau, the Yellow River Conservancy Commission, and the National Meteorological  
473 Information Center for providing the hydrological and meteorological data. We thank Jianjun  
474 Zhang for help in doing some figures and Zheng Ning for collecting the hydrological data.

475

#### 476 **References**

477 Achete, F.M., van der Wegen, M., Roelvink, D., and Jaffe, B.: A 2-D process-based model  
478 for suspended sediment dynamics: a first step towards ecological modeling, Hydrol.  
479 Earth Syst. Sci., 19, 2837-2857, 2015.

480 Beechie, T. J., Sear, D.A., Olden, J.D., Pess, G.R., Buffington, J.M., Moir, H., Roni, P., and  
481 Pollock, M.M.: Process-based principles for restoring river ecosystems, Bioscience, 60,  
482 209-222, 2010.

483 Chen, Y.P., Wang, K.B., Lin, Y.S., Shi, W.Y., Song, Y., and He, X.H.: Balancing green and  
484 grain trade, Nat. Geosci., 8, 739-741, 2015.

485 Cohen, S., Kettner, A.J., and Syvitski, J.P.M.: Global suspended sediment and water  
486 discharge dynamics between 1960 and 2010: continental trends and intra-basin



- 487 sensitivity, *Glob. Planet. Chang.*, 115, 44-58, 2014.
- 488 Farley, K.A., Jobbágy, E.G., and Jackson, R.B.: Effects of afforestation on water yield: a  
489 global synthesis with implications for policy, *Glob. Chang. Biol.*, 11, 1565-1576, 2005.
- 490 Hirsch, R.M., Slack, J.R., and Smith, R.A.: Techniques of trend analysis for monthly water  
491 quality data, *Water Resour. Res.*, 18, 107-121, 1982.
- 492 Kendall, M.G.: *Rank Correlation Measures*, Charles Griffin, London, UK, 1975.
- 493 Liu, X.Y., Yang, S.T., Dang, S.Z., Luo, Y., Li, X.Y., and Zhou X.: Response of sediment  
494 yield to vegetation restoration at a large spatial scale in the Loess Plateau, *Sci. China  
495 Tech. Sci.*, 57, 1482-1489, 2014
- 496 Mann, H.B.: Nonparametric tests against trend, *Econometrica*, 13(3), 245-259, 1945.
- 497 Ma, X., Lu, X.X., van Noordwijk, M., Li, J.T., and Xu, J.C.: Attribution of climate change,  
498 vegetation restoration, and engineering measures to the reduction of suspended sediment  
499 in the Kejie catchment, southwest China, *Hydrol. Earth Syst. Sci.*, 18, 1979-1994, 2014.
- 500 McVicar, T.R., Li, L.T., Van Niel, T.G., Zhang, L., Li, R., Yang, Q.K., Zhang, X.P., Mu, X.M.,  
501 Wen, Z.M., Liu, W.Z., Zhao, Y.A., Liu, Z.H., and Gao, P.: Developing a decision support  
502 tool for China's re-vegetation program: simulating regional impacts of afforestation on  
503 average annual streamflow in the Loess Plateau, *For. Ecol. Manag.*, 251, 65-81, 2007.
- 504 Miao, C.Y., Ni, J.R., and Borthwick, A.G.L.: Recent changes of water discharge and  
505 sediment load in the Yellow River basin, China, *Prog. Phys. Geogr.*, 34, 541-561, 2010.
- 506 Miao, C.Y., Ni, J.R., Borthwick, A.G.L, and Yang, L.: A preliminary estimate of human and  
507 natural contributions to the changes in water discharge and sediment load in the Yellow  
508 River, *Glob. Planet. Chang.*, 76, 196-205, 2011.



- 509 Milliman, J.D., Farnsworth, K.L., Jones, P.D., Xu, K.H., and Smith, L.C.: Climatic and  
510 anthropogenic factors affecting river discharge to the global ocean, 1951-2000, Glob.  
511 Planet. Chang., 62, 187-194, 2008.
- 512 Milly, P.C.D., Dunne, K.A., and Vecchia, A.V.: Global pattern of trends in streamflow and  
513 water availability in a changing climate, Nature, 438, 347-350, 2005.
- 514 Morera, S.B., Condom, T., Vauchel, P., Guyot, J.-L., Galvez, C., and Crave, A.: Pertinent  
515 spatio-temporal scale of observation to understand suspended sediment yield control  
516 factors in the Andean region: the case of the Santa River (Peru), Hydrol. Earth Syst. Sci.,  
517 17, 4641-4657, 2013.
- 518 Mutema, M., Chaplot, V., Jewitt, G., Chivenge, P., and Blöschl, G.: Annual water, sediment,  
519 nutrient, and organic carbon fluxes in river basins: A global meta-analysis as a function  
520 of scale, Water Resour. Res., 51, doi:10.1002/2014WR016668, 2015.
- 521 Nilsson, C., Reidy, C.A., Dynesius, M., and Revenga, C.: Fragmentation and flow regulation  
522 of the world's large river systems, Science, 308, 405-408, 2005.
- 523 Rustomji, P., Zhang, X.P., Hairsine, P.B., Zhang, L., and Zhao J.: River sediment load and  
524 concentration responses to changes in hydrology and catchment management in the  
525 Loess Plateau of China, Water Resour. Res., 44, W00A04, doi:10.1029/2007WR006656,  
526 2008.
- 527 Sen, P.K., 1968. Estimates of the regression coefficient based on Kendall's tau, J. Am. Stat.  
528 Assoc., 63, 1379-1389.
- 529 Song, C.L., Wang, G.X., Sun, X.Y., Chang, R.Y., and Mao, T.X.: Control factors and scale  
530 analysis of annual river water, sediments and carbon transport in China, Sci. Rep.,





- 531 6:25963, doi:10.1038/srep25963, 2016.
- 532 Sun, Q.H., Miao, C.Y., Duan, Q.Y., and Wang, Y.F.: Temperature and precipitation changes  
533 over the Loess Plateau between 1961 and 2011, based on high-density gauge  
534 observations, *Glob. Planet. Chang.*, 132, 1-10, 2015.
- 535 Sun, W.Y., Song, X.Y., Mu, X.M., Gao, P., Wang, F., and Zhao, G.J.: Spatiotemporal  
536 vegetation cover variations associated with climate change and ecological restoration in  
537 the Loess Plateau, *Agric. For. Meteorol.*, 209, 87-99, 2015.
- 538 Syvitski, J.P.M.: Supply and flux of sediment along hydrological pathways: Research for the  
539 21st century, *Glob. Planet. Chang.*, 39, 1-11, 2003.
- 540 Syvitski, J.P.M., Vörösmarty, C.J., Kettner, A.J., and Green, P.: Impact of humans on the flux  
541 of terrestrial sediment to the global coastal ocean, *Science*, 308, 376-380, 2005.
- 542 Walling, D.E. and Fang, D.: Recent trends in the suspended sediment loads of the world  
543 rivers, *Glob. Planet. Chang.*, 39, 111-126, 2003.
- 544 Walling, D.E.: Human impact on land-ocean sediment transfer by the world's rivers,  
545 *Geomorphology*, 79, 192-216, 2006.
- 546 Wang, H.J., Saito, Y., Zhang, Y., Bi, N.S., Sun, X.X., and Yang, Z.S.: Recent changes of  
547 sediment flux to the western Pacific Ocean from major rivers in east and south-east Asia,  
548 *Earth Sci. Rev.*, 108, 80-100, 2011.
- 549 Wang, S., Fu, B., Piao, S., Lü, Y., Philippe, C., Feng, X., and Wang, Y.: Reduced sediment  
550 transport in the Yellow River due to anthropogenic changes, *Nat. Geosci.*, 9, 38-41,  
551 2016.
- 552 Yao, W.Y., Xu, J.H., and Ran, D.C.: Assessment of Changing Trends in Streamflow and



- 553 Sediment Fluxes in the Yellow River Basin, Yellow River Water Conservancy Press,  
554 Zhengzhou, China, 2011 (in Chinese).
- 555 Yue, S. and Wang, C.Y.: Applicability of pre-whitening to eliminate the influence of serial  
556 correlation on the Mann-Kendall test, *Water Resour. Res.*, 38, 1068,  
557 doi:10.1029/2001WR000861, 2002.
- 558 Zhang, B.Q., He, C.S., Burnham, M., and Zhang, L.H.: Evaluating the coupling effects of  
559 climate aridity and vegetation restoration on soil erosion over the Loess Plateau in China,  
560 *Sci. Total Environ.*, 539, 436-449, 2016.
- 561 Zhang, L., Zhao, F.F., Chen, Y., and Dixon, R.N.M.: Estimating effects of plantation  
562 expansion and climate variability on streamflow for catchments in Australia, *Water*  
563 *Resour. Res.*, 47, W12539, doi:10.1029/2011WR010711, 2011.
- 564 Zhao, G.J., Mu, X.M., Jiao, J.Y., An, Z.F., Klik, A., Wang, F., Jiao, F., Yue, X.L., Gao, P., and  
565 Sun, W.Y.: Evidence and causes of spatiotemporal changes in runoff and sediment yield  
566 on the Chinese Loess Plateau, *Land Degrad. Dev.*, doi:10.1002/ldr.2534, 2016.  
567



568 **Figure captions**

569 **Figure 1.** Location of the studied catchments in the Coarse Sandy Hilly Catchments

570 (CSHC) region within the Loess Plateau.

571 **Figure 2.** Annual precipitation, streamflow and sediment load for the whole CSHC region

572 during 1961-2011.

573 **Figure 3.** The changes of (a) land use, (b) soil and water conservation measures area, (c)

574 vegetation cover and (d) LAI in the study area.

575 **Figure 4.** The changes of (a) precipitation, (b) streamflow, (c) sediment yield, (d) sediment

576 concentration and (e) sediment coefficient during different stages (1961-1969,

577 1970-1999 and 2000-2011).

578 **Figure 5.** Contributions of precipitation and land use/cover to reductions of sediment load

579 from (a) reference period (P1) to period-2 (P2), (b) reference period (P1) to period-3 (P3)

580 and (c) period-2 (P2) to period-3 (P3).

581 **Figure 6.** The relationship between annual precipitation and sediment yield during the

582 reference period (1961-1969).

583 **Figure 7.** The relationship between annual precipitation and sediment yield during the

584 period-2 (1970-1999).

585 **Figure 8.** The relationship between annual sediment yield and precipitation during the

586 period-3 (2000-2011).

587 **Figure 9.** Daily precipitation and sediment load of the Yanhe catchment during rainy

588 season (May-October) in (a) 2003 and (b) 2004.

589 **Figure 10.** Relationships between the sediment coefficient and percentage of the area

590 affected by soil and water conservation measures in the catchments. The data points

591 represent the average values of 1960s, 1970s, 1980s, 1990s, and 2000s.



**Table 1.** Long-term hydrometeorological characteristics (1961-2011) and leaf area index (LAI) (1982-2011) of the studied catchments in the Loess Plateau.

ID	Catchment	Gauging station	Area (km <sup>2</sup> )	Annual average					
				P (mm)	Q (mm)	SSY (t km <sup>-2</sup> )	SC (kg m <sup>-3</sup> )	C <sub>s</sub> (t km <sup>-2</sup> mm <sup>-1</sup> )	LAI
1	Huangfu	Huangfu	3175	388.95	36.34	11608.86	275.90	27.35	0.351
2	Gushan	Gaoshiya	1263	422.49	49.55	12398.68	189.57	25.98	0.364
3	Kuye	Wenjiachuan	8515	394.63	59.25	9099.60	114.99	21.17	0.324
4	Tuwei	Gaojiachuan	3253	402.82	97.53	4454.47	38.44	10.16	0.363
5	Jialu	Shenjiawan	1121	445.51	49.22	9645.19	142.19	20.03	0.365
6	Wuding	Baijiachuan	29662	384.32	36.39	3089.61	74.09	7.67	0.371
7	Qingjian	Yanchuan	3468	485.58	38.93	8747.17	190.57	17.35	0.905
8	Yanhe	Ganguyi	5891	516.09	34.08	6604.90	166.31	12.45	1.623
9	Shiwang	Dacun	2141	572.16	32.99	798.89	20.32	1.31	2.158
10	Qushui	Linjiaping	1873	469.02	34.83	7818.21	185.79	15.75	0.632
11	Sanchuan	Houdacheng	4102	486.23	50.37	3444.56	53.39	6.63	1.242
12	Quchan	Peigou	1023	539.73	30.24	7492.57	192.01	13.68	0.622
13	Xinshui	Daning	3992	529.96	29.22	3004.96	86.81	5.23	1.141
14	Zhouchuan	Jixian	436	530.06	30.13	4951.15	107.99	8.55	0.774
15	CSHC	Toudaoguai and Longmen	129654	437.27	33.30	3988.04	102.42	8.73	0.523



**Table 2.** Mann-Kendall trend analysis results for the annual precipitation ( $P$ ), streamflow ( $Q$ ), specific sediment yield ( $SSY$ ), sediment concentration ( $SC$ ), sediment coefficient ( $C_s$ ) during 1961-2011.

Catchment	$P$		$Q$		$SSY$		$SC$		$C_s$	
	$Z$	$\beta$ (mm yr <sup>-1</sup> )	$Z$	$\beta$ (mm yr <sup>-1</sup> )	$Z$	$\beta$ (t km <sup>2</sup> yr <sup>-1</sup> )	$Z$	$\beta$ (kg m <sup>-3</sup> yr <sup>-1</sup> )	$Z$	$\beta$ (t km <sup>-2</sup> mm <sup>-1</sup> yr <sup>-1</sup> )
Huangfu	-0.57 <sup>ns</sup>	-0.52	-4.82***	-0.99	-4.50***	-323.24	-1.97*	-2.58	-4.71***	-0.80
Gushan	-0.78 <sup>ns</sup>	-1.16	-5.02***	-1.47	-4.90***	-398.82	-3.75***	-3.92	-5.15***	-0.87
Kuye	-0.49 <sup>ns</sup>	-0.37	-5.98***	-1.66	-5.41***	-288.83	-4.61***	-3.22	-5.60***	-0.63
Tuwei	-0.24 <sup>ns</sup>	-0.27	-7.88***	-1.57	-5.20***	-130.34	-4.37***	-0.98	-5.59***	-0.30
Jialu	0.19 <sup>ns</sup>	0.26	-7.55***	-1.42	-5.36***	-298.10	-3.80***	-3.89	-5.60***	-0.69
Wuding	-0.39 <sup>ns</sup>	-0.37	-6.60***	-0.54	-4.55***	-79.19	-3.33***	-1.35	-4.94***	-0.20
Qingjian	-0.73 <sup>ns</sup>	-0.56	-2.06*	-0.24	-3.01**	-138.54	-3.09**	-3.53	-2.73**	-0.30
Yanhe	-1.19 <sup>ns</sup>	-1.17	-3.22**	-0.34	-3.36***	-115.18	-3.30***	-3.07	-3.10**	-0.22
Shiwang	-1.20 <sup>ns</sup>	-1.50	-4.01***	-0.61	-6.26***	-26.47	-5.43***	-0.69	-6.12***	-0.04
Qushui	-0.28 <sup>ns</sup>	-0.35	-5.80***	-0.97	-6.98***	-290.44	-5.00***	-4.00	-5.98***	-0.55
Sanchuan	-1.43 <sup>ns</sup>	-1.71	-6.09***	-0.96	-5.35***	-108.69	-5.13***	-1.60	-5.99***	-0.21
Quchan	-0.94 <sup>ns</sup>	-1.14	-3.23**	-0.42	-3.65***	-173.16	-3.72***	-4.12	-3.46***	-0.29
Xinshui	-2.37*	-2.71	-5.57***	-0.70	-5.92***	-106.30	-3.77***	-1.92	-5.60***	-0.19
Zhouchuan	-2.21*	-2.48	-7.20***	-0.79	-5.86***	-183.49	-6.73***	-4.70	-7.12***	-0.35
CSHC	-0.67 <sup>ns</sup>	-0.55	-5.91***	-0.85	-5.70***	-131.52	-4.26***	-2.06	-5.67***	-0.27

<sup>a</sup> \*\*\*, \*\* and \* indicate the significance levels of 0.001, 0.01 and 0.05, respectively. ns indicates the significance levels exceeds 0.05.

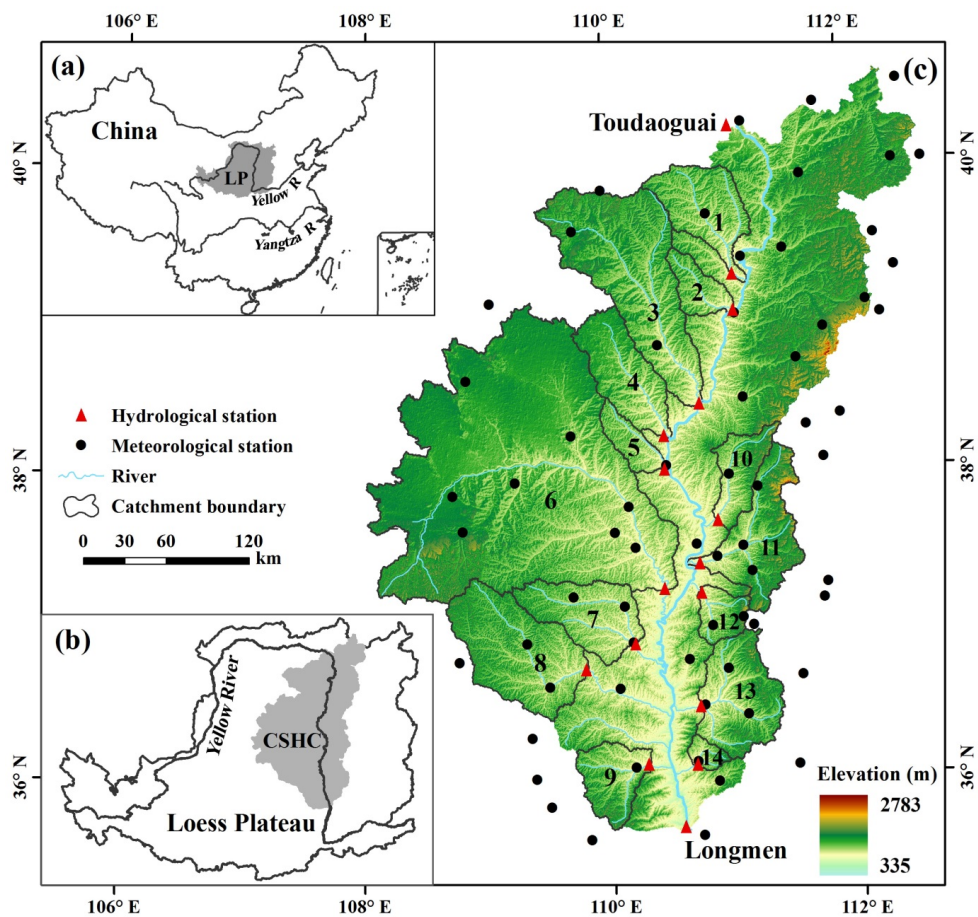


**Table 3.** The linear regression equations between annual precipitation and sediment load during three stages (1961-1969, 1970-1999 and 2000-2011).

ID	Catchment	Reference period (1961-1969)			Period-2 (1970-1999)			Period-3 (2000-2011)		
		Regression equation	$R^2$	$p$	Regression equation	$R^2$	$p$	Regression equation	$R^2$	$p$
1	Huangfu	$y = 85.10x - 9752.3$	0.72	0.004	$y = 88.67x - 12773$	0.37	0.000	$y = 10.61x - 1386.4$	0.11	0.296
2	Gushan	$y = 93.16x - 11606$	0.85	0.000	$y = 84.91x - 12876$	0.31	0.001	$y = 6.79x - 441.92$	0.11	0.291
3	Kuye	$y = 66.42x - 5353.1$	0.55	0.022	$y = 57.86x - 7048.9$	0.28	0.002	$y = 1.95x - 33.53$	0.06	0.435
4	Tuwei	$y = 34.35x - 2830.4$	0.84	0.001	$y = 23.90x - 2913.2$	0.16	0.031	$y = -2.05x + 1076.9$	0.05	0.469
5	Jialu	$y = 90.23x - 7626.1$	0.75	0.005	$y = 47.31x - 6155.7$	0.08	0.128	$y = 9.98x - 1713.1$	0.07	0.405
6	Wuding	$y = 21.76x - 649.01$	0.40	0.068	$y = 16.96x - 1918.7$	0.24	0.006	$y = 8.25x - 1291.3$	0.25	0.101
7	Qingjian	$y = 49.75x - 5568.4$	0.27	0.154	$y = 37.74x - 3904.1$	0.20	0.014	$y = 8.15x - 580.79$	0.05	0.513
8	Yanhe	$y = 56.63x - 11559$	0.34	0.100	$y = 20.76x - 697.94$	0.13	0.053	$y = 4.12x + 900.6$	0.05	0.831
9	Shiwang	$y = 7.26x - 1255.3$	0.33	0.104	$y = 5.02x - 1193$	0.22	0.008	$y = -0.16x + 128.3$	0.02	0.667
10	Qiushui	$y = 63.64x - 5673.8$	0.47	0.043	$y = 42.20x - 6950$	0.22	0.008	$y = -8.14x + 4488.1$	0.03	0.564
11	Sanchuan	$y = 28.53x - 2109.1$	0.24	0.180	$y = 18.75x - 3458.8$	0.36	0.000	$y = -3.99x + 1901$	0.11	0.282
12	Quchan	$y = 39.87x - 1265.6$	0.25	0.258	$y = 20.51x + 60.83$	0.04	0.279	$y = -26.78x + 13294$	0.11	0.300
13	Xinshui	$y = 27.62x - 4923.5$	0.62	0.012	$y = 19.27x - 4077.4$	0.48	0.000	$y = 0.90x + 372.85$	0.01	0.777
14	Zhouchuan	$y = 51.41x - 8690.4$	0.36	0.090	$y = 42.27x - 10495$	0.28	0.003	$y = -1.05x + 666.84$	0.07	0.408
15	CSHC	$y = 33.13x - 4167.96$	0.60	0.015	$y = 20.34x - 2728.2$	0.27	0.003	$y = 2.03x + 174.09$	0.01	0.715

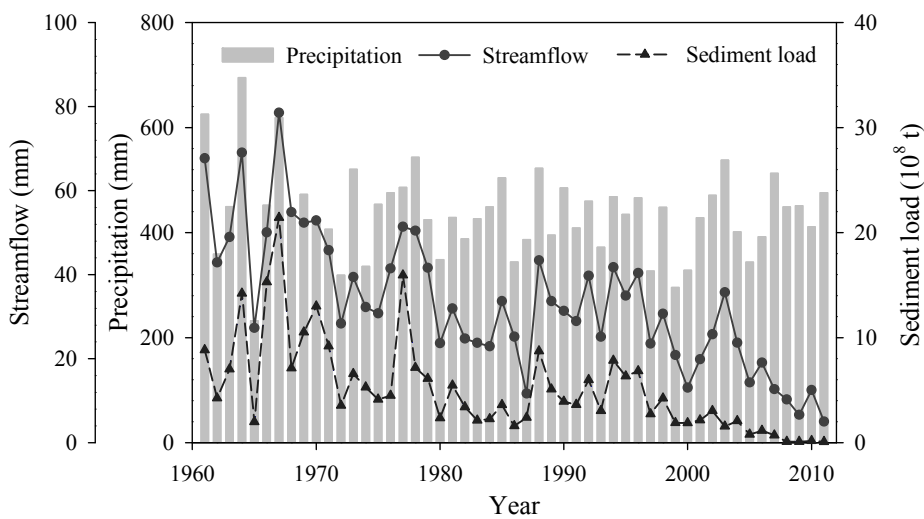
**Table 4.** Regression equations between the sediment coefficient and percentage of the area affected by soil and water conservation measures in the catchments.

ID	Catchment	Regression equation	$R^2$	$p$
1	Huangfu	$y = -0.67x + 45.88$	0.85	0.025
2	Gushan	$y = -0.90x + 46.66$	0.82	0.034
3	Kuye	$y = -0.83x + 38.32$	0.89	0.017
4	Tuwei	$y = -0.48x + 19.94$	0.98	0.002
5	Jialu	$y = -1.20x + 53.20$	0.97	0.002
6	Wuding	$y = -0.31x + 16.92$	0.97	0.003
7	Qingjian	$y = -0.31x + 24.70$	0.48	0.193
8	Yanhe	$y = -0.26x + 18.54$	0.79	0.045
9	Shiwang	$y = -0.15x + 3.01$	0.87	0.020
10	Qiushui	$y = -0.87x + 35.69$	0.80	0.040
11	Sanchuan	$y = -0.28x + 13.32$	0.78	0.046
12	Quchan	$y = -0.29x + 21.02$	0.52	0.169
13	Xinshui	$y = -0.20x + 8.63$	0.72	0.069
14	Zhouchuan	$y = -0.61x + 17.89$	0.61	0.118
15	CSHC	$y = -0.54x + 17.74$	0.99	0.000

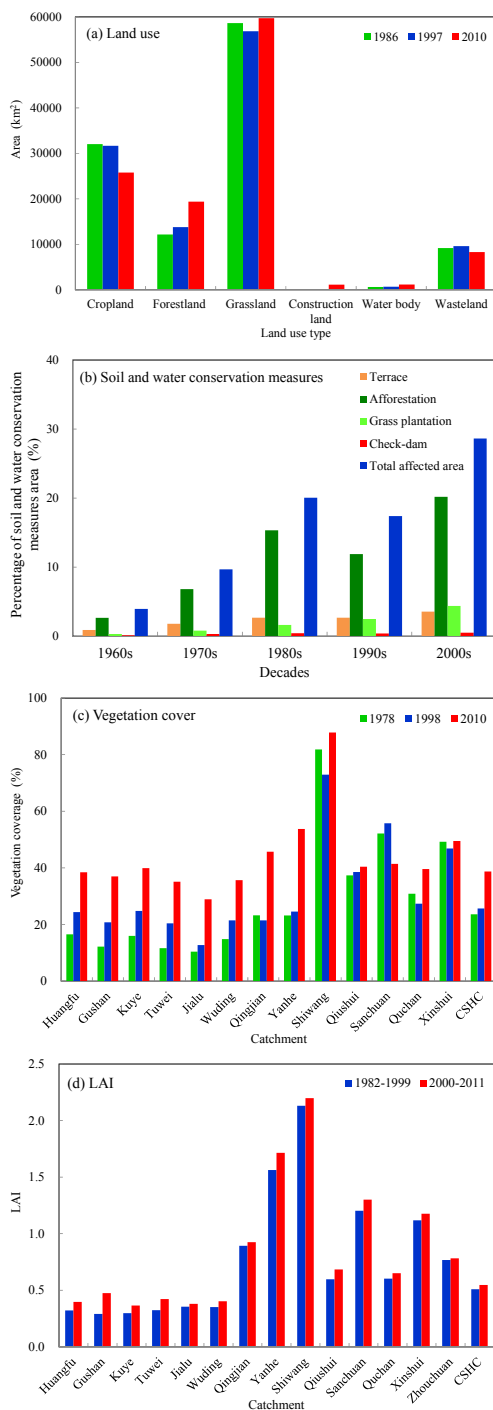


**Figure 1.** Location of the studied catchments in the Coarse Sandy Hilly Catchments (CSHC) region within the Loess Plateau.

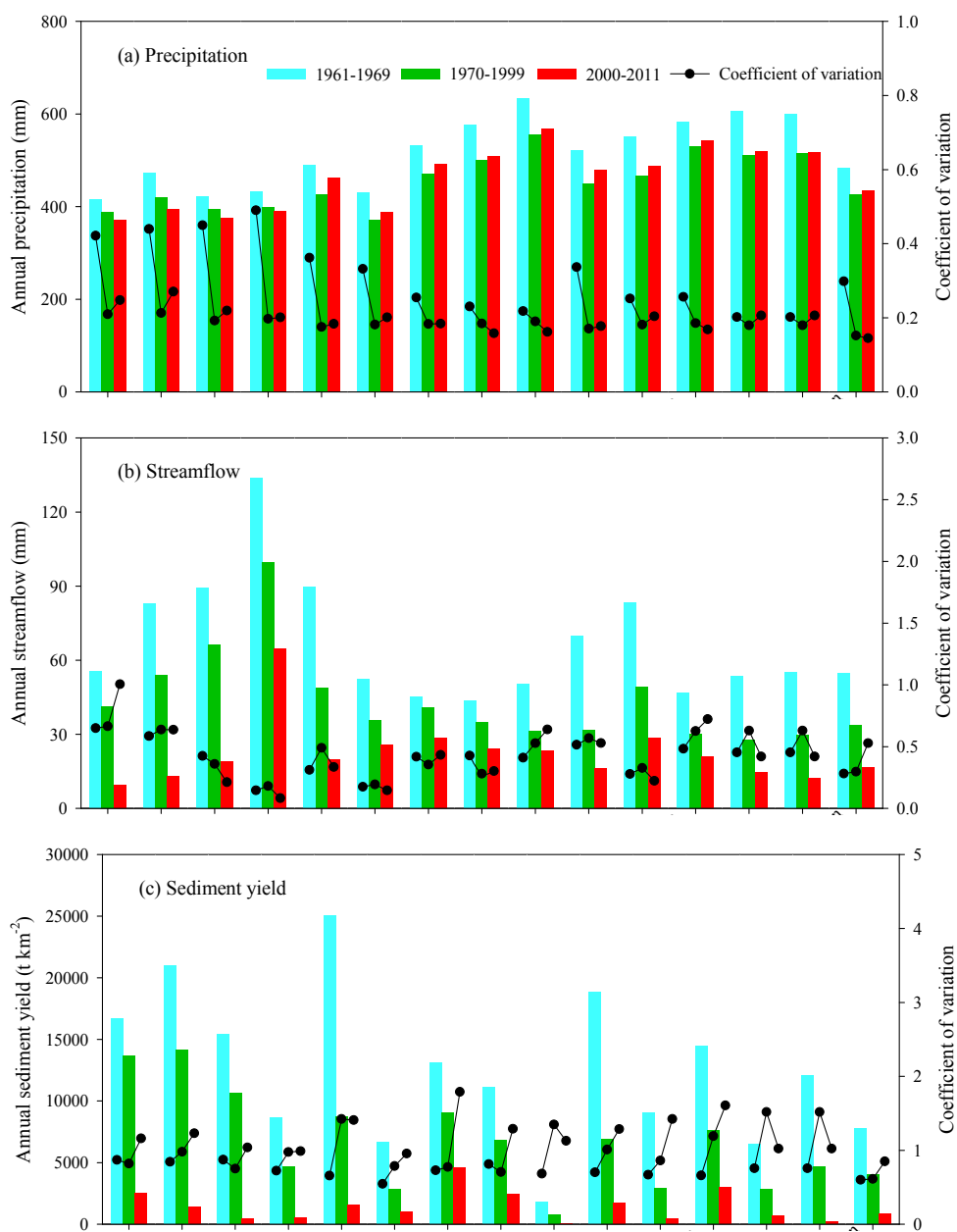




**Figure 2.** Annual precipitation, streamflow and sediment load for the whole CSHC region during 1961-2011.



**Figure 3.** The changes of (a) land use, (b) soil and water conservation measures area, (c) vegetation cover and (d) LAI in the study area.



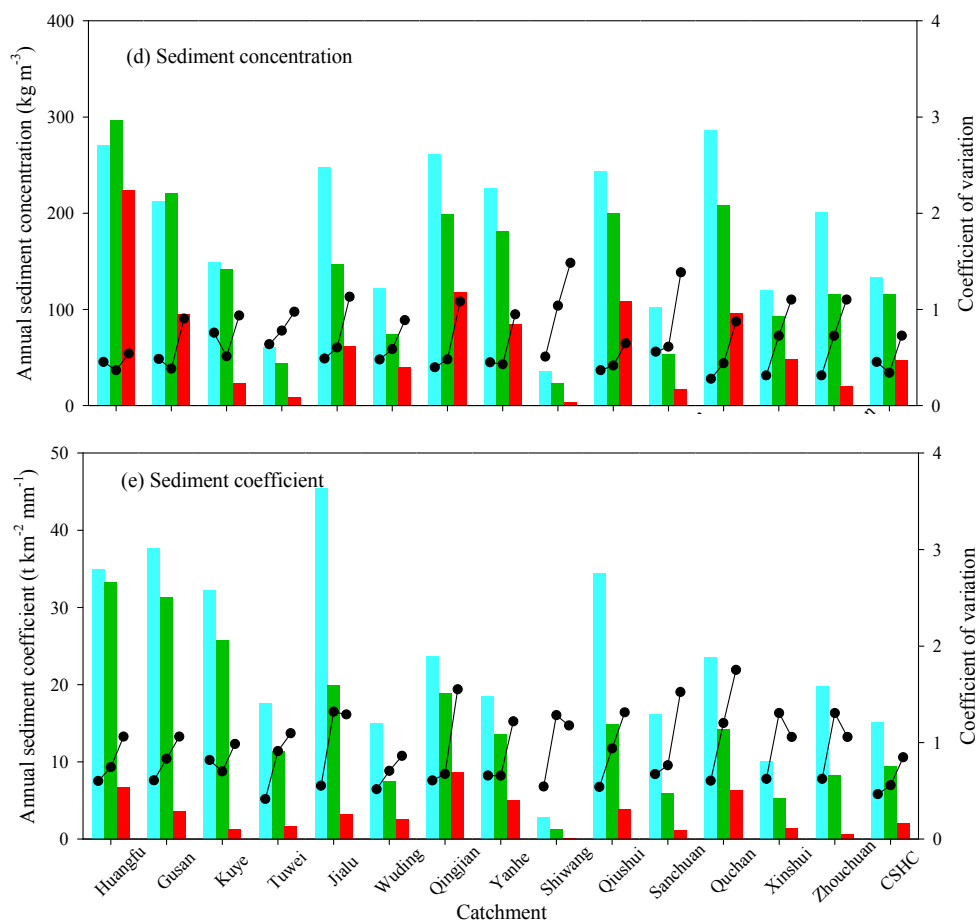


**Figure 4.** The changes of (a) precipitation, (b) streamflow, (c) sediment yield, (d) sediment concentration and (e) sediment coefficient during different stages (1961-1969, 1970-1999 and 2000-2011).

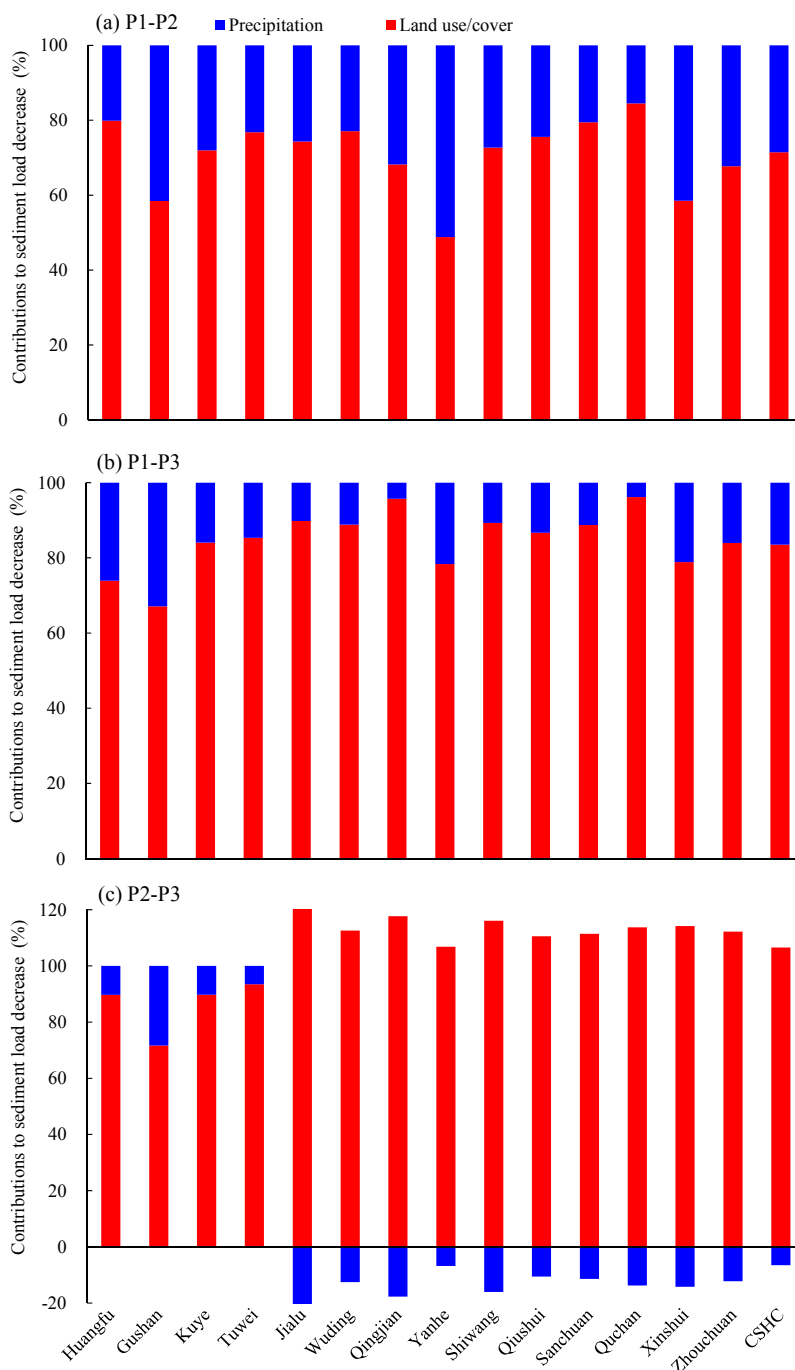


**Figure 5.** Contributions of precipitation and land use/cover to reductions of sediment load from (a) reference period (P1) to period-2 (P2), (b) reference period (P1) to period-3 (P3) and (c) period-2 (P2) to period-3 (P3).

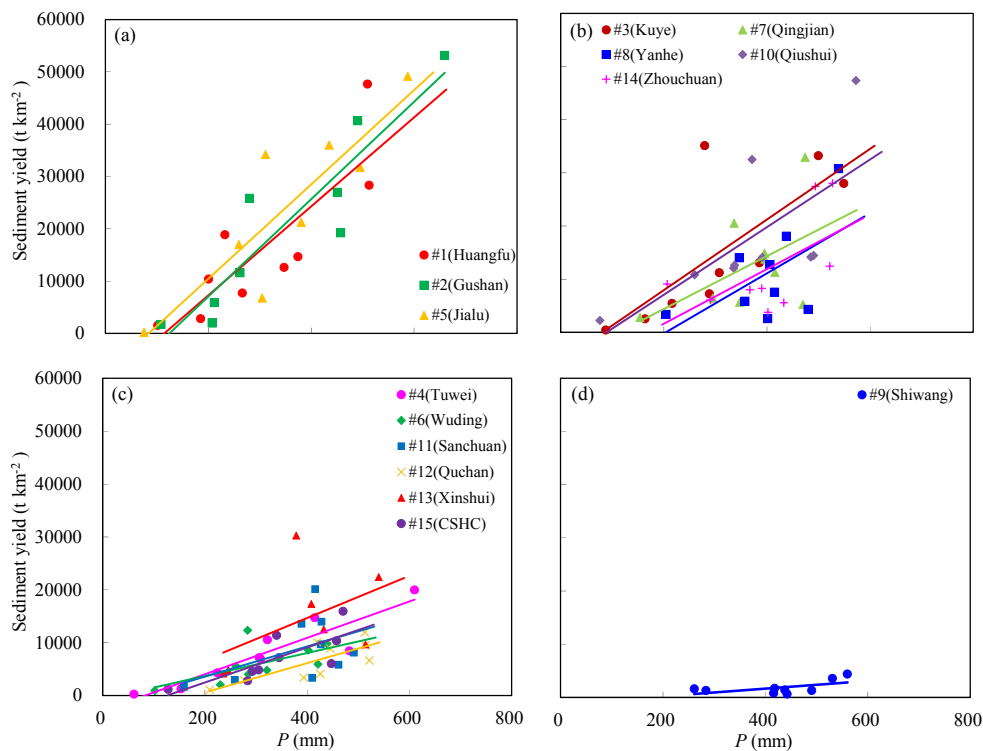


**Figure 6.** The relationship between annual precipitation and sediment yield during the reference period (1961-1969).

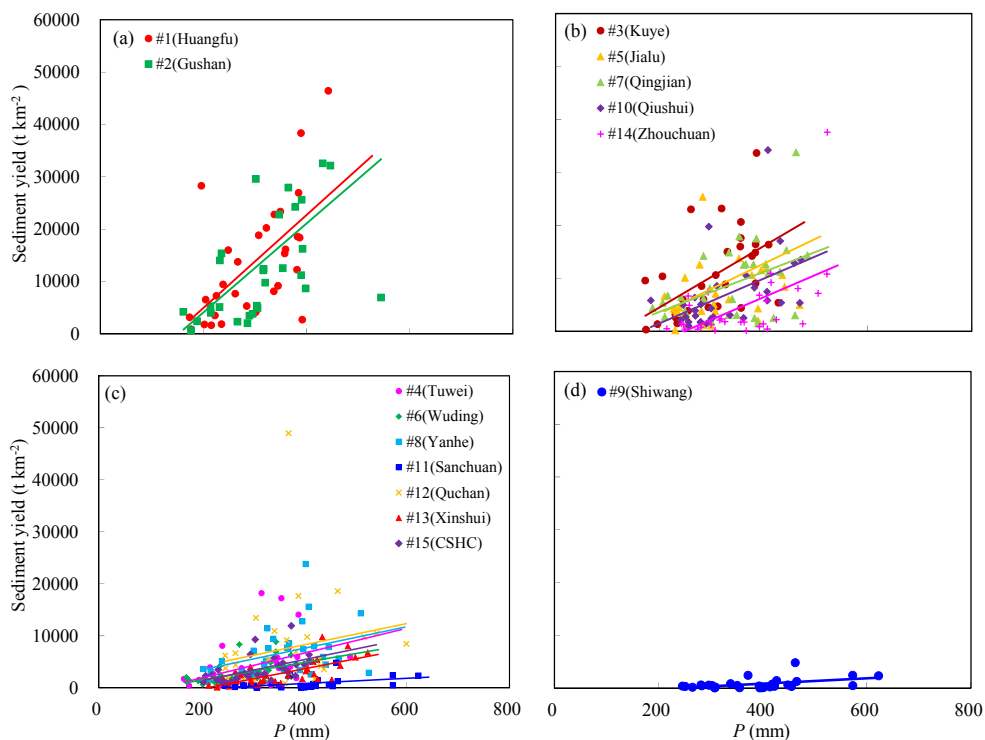


**Figure 7.** The relationship between annual precipitation and sediment yield during the period-2 (1970-1999).

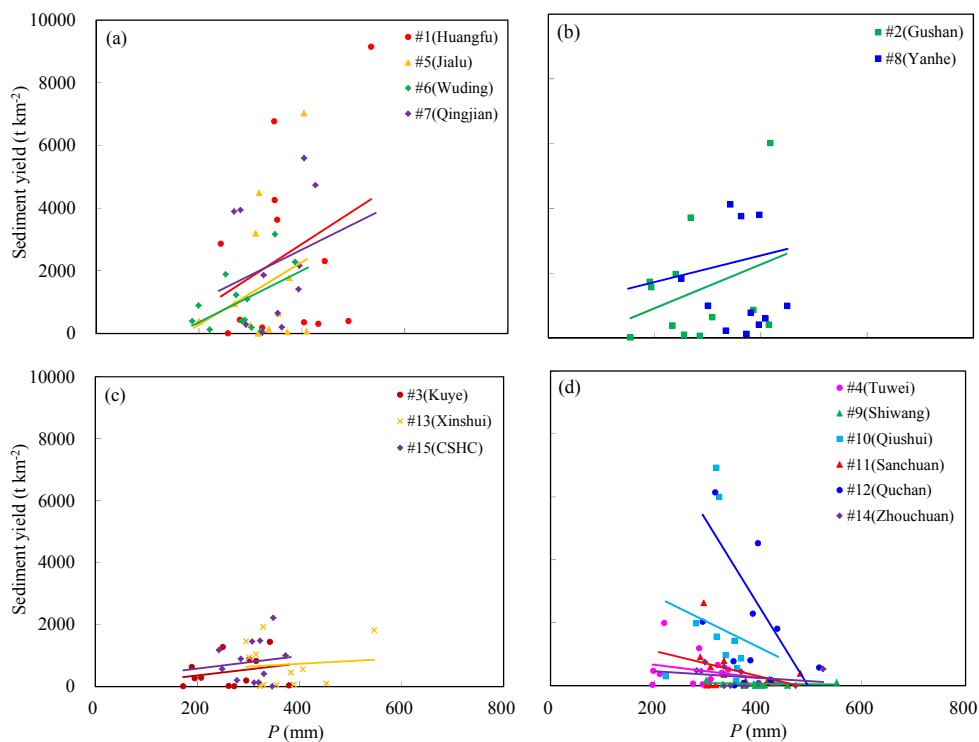


**Figure 8.** The relationship between annual sediment yield and precipitation during the period-3 (2000-2011).



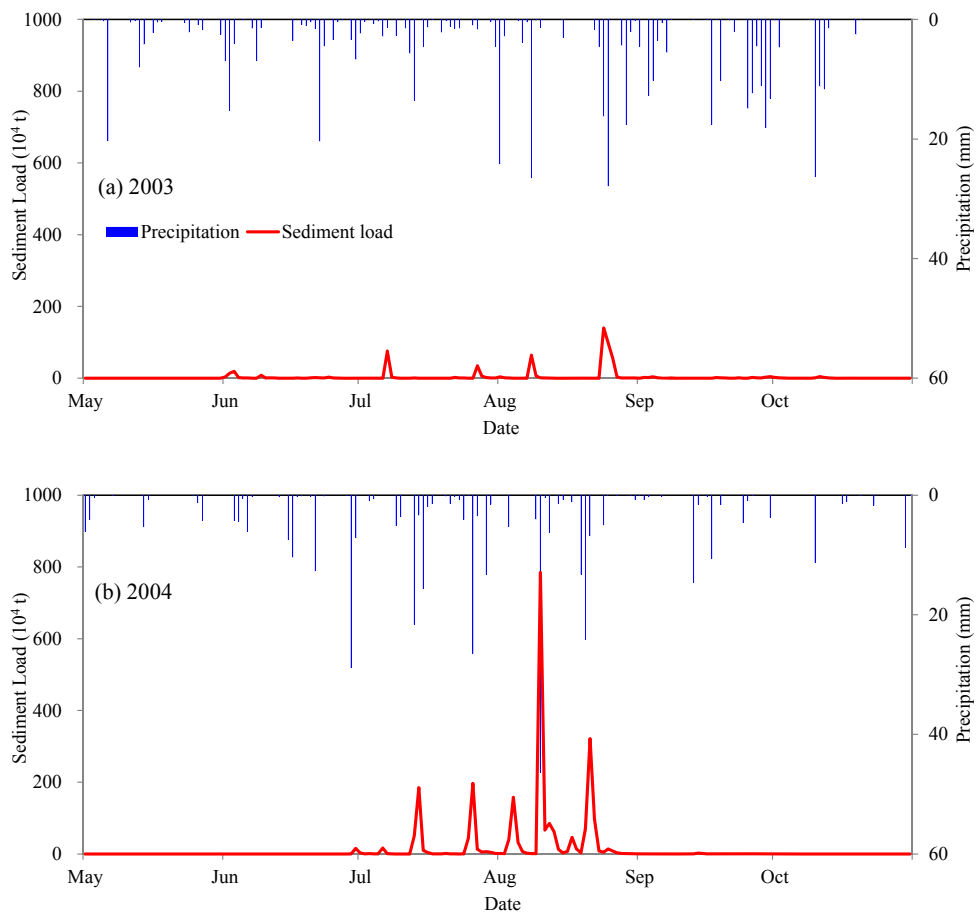


**Figure 9.** Daily precipitation and sediment load of the Yanhe catchment during rainy season (May-October) in (a) 2003 and (b) 2004.

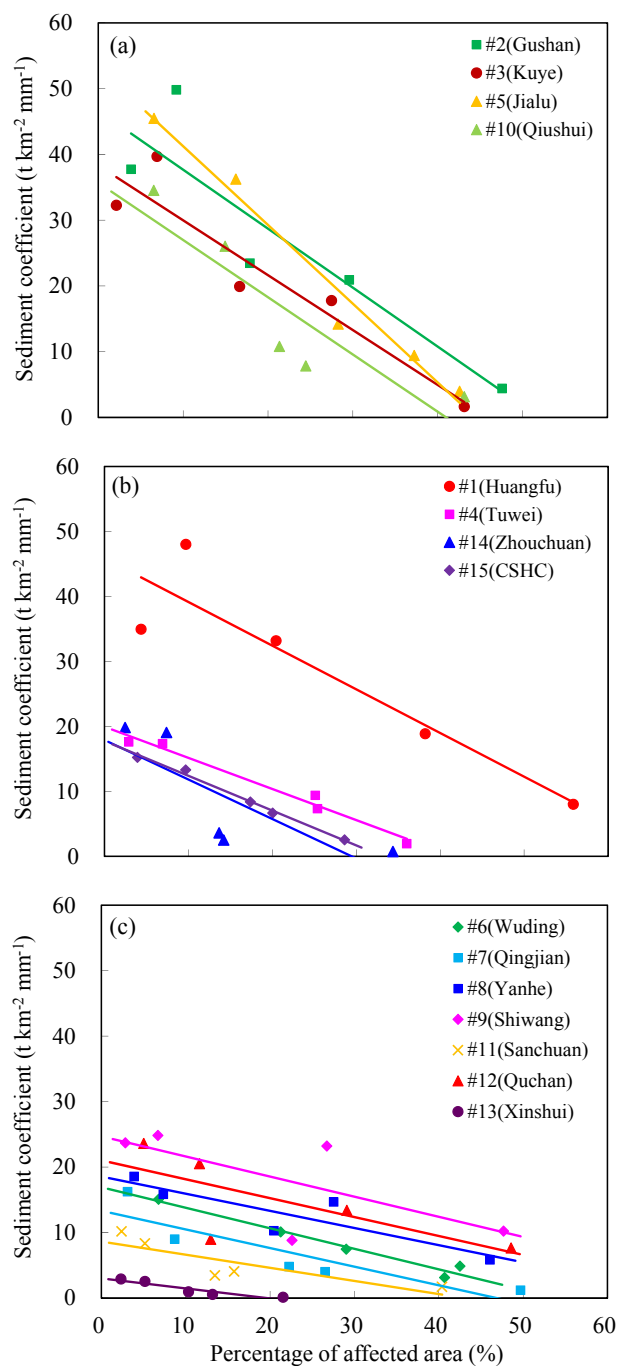


**Figure 10.** Relationships between the sediment coefficient and percentage of the area affected by soil and water conservation measures in the catchments. The data points represent the average values of 1960s, 1970s, 1980s, 1990s, and 2000s.